Front. Mater. Sci. 2014, 8(1): 72–86
DOI 10.1007/s11706-014-0234-z

RESEARCH ARTICLE

Time-sequential changes of differentially expressed miRNAs during the process of anterior lumbar interbody fusion using equine bone protein extract, rhBMP-2 and autograft

Da-Fu CHEN [1*], Zhi-Yu ZHOU [2,5*], Xue-Jun DAI [2*], Man-Man GAO[2], Bao-Ding HUANG[2], Tang-Zhao LIANG[2], Rui SHI[1], Li-Jin ZOU[3], Hai-Sheng LI[4], Cody BÜNGER[4], Wei TIAN (✉)[1], and Xue-Nong ZOU (✉)[2]

1 Laboratory of Bone Tissue Engineering, Beijing Research Institute of Traumatology and Orthopaedics, Beijing Jishuitan Hospital, Beijing 100035, China
2 Department of Spine Surgery/Orthopaedic Research Institute, The First Affiliated Hospital of Sun Yat-sen University, Guangzhou 510080, China
3 Department of Surgery, the First Affiliated Hospital of Nanchang University, Nanchang 330006, China
4 Orthopaedic Research Laboratory/The Institute of Clinical Medicine, Aarhus University Hospital, DK-8000 Aarhus, Denmark
5 Medicine School, Shenzhen University, Shenzhen 518060, China

© Higher Education Press and Springer-Verlag Berlin Heidelberg 2014

ABSTRACT: The precise mechanism of bone regeneration in different bone graft substitutes has been well studied in recent researches. However, miRNAs regulation of the bone formation has been always mysterious. We developed the anterior lumbar interbody fusion (ALIF) model in pigs using equine bone protein extract (BPE), recombinant human bone morphogenetic protein-2 (rhBMP-2) on an absorbable collagen sponge (ACS), and autograft as bone graft substitute, respectively. The miRNA and gene expression profiles of different bone graft materials were examined using microarray technology and data analysis, including self-organizing maps, KEGG pathway and Biological process GO analyses. We then jointly analyzed miRNA and mRNA profiles of the bone fusion tissue at different time points respectively. Results showed that miRNAs, including let-7, miR-129, miR-21, miR-133, miR-140, miR-146, miR-184, and miR-224, were involved in the regulation of the immune and inflammation response, which provided suitable inflammatory microenvironment for bone formation. At late stage, several miRNAs directly regulate SMAD4, Estrogen receptor 1 and 5-hydroxytryptamine (serotonin) receptor 2C for bone formation. It can be concluded that miRNAs play important roles in balancing the inflammation and bone formation.

KEYWORDS: miRNA; bone protein extract (BPE); recombinant human bone morphogenetic protein-2 (rhBMP-2); autograft

Contents

Received February 10, 2014; accepted March 5, 2014

E-mails: tianweijst@yahoo.com.cn (W.T.), zxnong@hotmail.com (X.N.Z.)

*D.F.C, Z.Y.Z and X.J.D. contributed equally to this work.

1 Introduction

MicroRNAs (miRNAs) represent a class of small, functional, noncoding RNAs of 19 to 23 nucleotides that regulate the transcription of messenger RNAs (mRNAs) in proteins. miRNAs are identified to target mRNA through 5′-seed sequences interacting with their regulatory elements mostly located in the 3′-untranslated region (3′-UTR) of the target mRNA. They play important roles in multiply biological and metabolic processes, including development, cell proliferation, differentiation, apoptosis and other metabolic processes [1].

In the past few years, reports on miRNAs related with the regulation of osteogenesis and bone remodeling have emerged and kept growing [2]. Several *in vitro* studies have verified that biomaterials could induce upregulation or downregulation of miRNAs. These miRNAs were triggered by various biomaterials including anorganic bovine bone [3], titanium [4–7], PerioGlas [8], collagen and silicate-based synthetic bone [9], calcium sulfate [10], zirconium oxide [7,11], and porous polyethylene [12]. However, all above *in vitro* studies were implemented on single cell line, which could not demonstrate the effects of miRNA-mediated regulation on osteogenesis and bone remodeling under the situation of complex micro-environment *in vivo*.

In our previous studies, we assessed the osteogenesis and bone micro-architecture in anterior lumbar interbody fusion (ALIF) in pigs using equine bone protein extracts (BPEs), recombinant human bone morphogenetic protein-2 (rhBMP-2)/absorbable collagen sponge, and autograft bone [13–14]. We further investigated the gene expression profile of different bone graft biomaterials using gene expression microarray. These studies revealed that equine BPE induced endochondral ossification via upregulation of cartilage-related genes, which exhibited a similar expression pattern with autograft bone. rhBMP-2 could recruit progenitor cells, proliferation and differentiation possibly by inducing various genes and then leads to preferable membranous ossification [15]. We also verified that some genes related to inflammation response changed in the bone healing process. More importantly, the expression of all these genes was dynamically variable with the time and different bone graft biomaterials. Therefore, some precise regulation systems definitely exist in bone regeneration. We hypothesized that miRNAs, one of epigenetic regulation factor, possibly involved in the process of bone regeneration.

Based on our previous ALIF model in pigs using equine BPE, rhBMP-2 on absorbable collagen sponge (ACS) and autograft bone [15], we further jointly analyzed miRNA and mRNA profiles of fusion mass at different time points by the use of miRNA and gene expression microarray technology in the present study. Time-sequential analyses of differentially expressed miRNAs could make us to better understand miRNA-mediated regulation and its target mRNAs on bone regeneration induced by different bone graft biomaterials.

2 Materials and methods

2.1 Animal model and observation

Eighteen Danish female landrace pigs, 3-month-old, weighing approximately 50 kg, was chosen in the present study. Each underwent a 3-level ALIF procedure at L3-4, L4-5, and L5-6 with posterior pedicle screw fixation under general anaesthesia, which maintained by inhalation of sevoflorane 3%–3.5% (Abbott Scandinavia AB, Solna, Sweden) and 0.5 mg fentanyl (Haldid®, Janssen-Cilag, Janssen Pharmaceutica, Beerse, Belgium) per hour. Firstly, a posterior midline incision from L3 to L6 was made and the facet joints were exposed bilaterally through paraspinal intramuscular approaches. Under fluoroscopic control, pedicle screws (5.0×30 mm, Diapason, Stryker® Spine, Cestas, France) were inserted. Autograft was then harvested from the left iliac crest. Through a left paramedian incision, the anterior lumbar spine was exposed by a retroperitoneal approach. After removal of L3-4, L4-5, and L5-6 discs with adjacent endplates, each level was randomly inserted into a custom-made polyetheretherketone (PEEK) interbody cage with 40 mg of equine BPE (COLLOSS® E; Ossacur AG, Oberstenfeld,

Germany), 3 mg rhBMP-2 dissolved on one quarter of ACS (INFUSE®; Medtronic-Sofamor Danek, Memphis TN), or 1.27 g (SD 0.060 g) of autograft bone. The pigs were housed individually with free access to water. Ampicillin 15,000 IE/kg (PenoVet; Boehringer Ingelheim Vetmedica A/S, Copenhagen, Denmark) was given before, during, and after the operation. Postoperatively, six animals were terminated at each time-point of 2, 4, or 8 weeks, using an overdose injection of pentobarbital (20 mg/kg). The spine from level L1 to S1 was taken, stripped of soft tissue, immediately frozen with liquid nitrogen, and stored at −80°C until examination.

All animal surgeries and experiments were complied with the Danish Law on Animal Experimentation and were approved by the Danish Ministry of Justice Ethical Committee, J.nr. 2004-561-898. The animal study was performed at the Institute of Clinical Medicine at Aarhus University.

2.2 Histology

The frozen vertebral bodies including the cage were cut transversally. Then the cages were cut in halves in the sagittal plane. The fusion mass in one half of the cage was for total RNA extraction. Another half of the cage and its containment were dehydrated in a graded series of ethanol (70%–99%) and embedded in polymethyl methacrylate (PMMA). Slices with a thickness of 7 μm were made on 2 levels in the sagittal plane with 400 μm between each level using a microtome (Polycut E, Reichert-Jung, Heidelberg, Germany). They were stained with Goldners-Trichrome for histological observation. The sections were observed under the light microscope to define new bone and fibrous tissue, as well as the fusion status.

2.3 Tissue preparation and RNA extraction

While cooled with liquid nitrogen, each tissue sample in the middle of the cage was taken by a curette and homogenized in TRIzol reagent (Invitrogen) using a mixer mill (Retsch, Germany). Total RNA extraction was done from each tissue sample according to the manufacturer's instructions. The RNA quality was confirmed by calculating the optical density (OD) 260/280 ratio ($OD_{260/280}$) via a spectrophotometer and its integrity was verified by agarose electrophoresis. The amount of RNA was determined by measuring absorbance at 260 nm.

RNA samples, extracted from BPE, rhBMP-2, or autograft bone in a cage at each time point respectively, were pooled in equal amounts for microarray experiments, which is a cost-effective approach for reducing effects from individuals and identifying the most common differences in gene and miRNA expression.

2.4 Gene microarray experiment

Gene-expression profiling was performed for each pooling RNA sample separately on the GeneChip® Porcine Genome Array (Affymetrix) at CapitalBio Corporation (Beijing, China) as described in detail in our previous study [15]. The protocol for microarray processing was carried out according to the GeneChip Expression Analysis Technical Manual (Affymetrix, Rev.5, Part number 701021). In brief, 1 μg of total RNA was first reverse transcribed using the T7-Oligo Promoter Primer in the first-strand cDNA synthesis. Following RNase H and DNA polymerase mediated second-strand cDNA synthesis; the double-stranded cDNA was used for *in vitro* transcription. This reaction was carried out in the presence of T7 RNA polymerase and the biotinylated deoxyribonucleoside triphosphates (dNTPs), incubated overnight at 37°C for RNA amplification and biotin labeling. The labeled RNA was then fragmented and hybridized to the array for 16 h at 45°C with rotation. After hybridization, the arrays were washed and stained with streptavidin–phycoerythrin in a GeneChip® Fluidics Station 450 (Affymetrix). The hybridized microarrays were scanned using the GeneChip® Scanner 3000 and converted into TIFF images, in preparation for analysis.

2.5 miRNA microarray experiment

Total RNA samples were analyzed by CapitalBio Corporation (Beijing, China) for miRNA microarray experiments. miRNA expression profiling was performed for each pooling RNA sample separately on the GeneChip® miRNA 2.0 Array (Affymetrix) at CapitalBio Corporation. The individual oligonucleotide probe was printed in triplicate on chemically modified glass slides in a 21×21 spot configuration of each subarray. The spot diameter was 130 μm, and distance from center to center was 185 μm. miRNAs were enriched from total RNA extracted from each pooling RNA sample with mirVana miRNA Isolation Kit (Ambion, Foster City, CA, USA) and labeled with mirVana Array Labeling Kit (Ambion). Labeled miRNAs were used for hybridization on each miRNA microarray containing 15,644 mature miRNA probes derived from the Sanger miRBase miRNA 15.0 (http://microrna.sanger.ac.

uk) in triplicate, corresponding to 1,105 human, 722 mouse, 389 rat, and 189 porcine miRNAs, to determine differential expression among BPE, rhBMP-2 and autograft samples. This procedure was repeated twice.

Procedures were performed as described in detail on the website of CapitalBio (http://www.capitalbio.com). Briefly, the miRNA microarray from CapitalBio Corporation was single-channel fluorescence chip; all oligonucleotide probes were labeled with Cy3 fluorescent dyes (green color). Fluorescence scanning used a double-channel laser scanner (LuxScan 10K/A, CapitalBio). Then, the figure signal was transformed to digital signal using image analysis software (LuxScan 3.0, CapitalBio). Signal intensities for each spot were calculated by subtracting local background from total intensities.

2.6 Data processing and analysis

Raw data were normalized and analyzed using the Significance Analysis of Microarrays (SAM; version 2.1, Stanford University, CA, USA) software. In the present study, differentially expressed miRNAs were defined as following standards: Fold Change $\geqslant 2$ or $\leqslant 0.5$, and q-value (%) $\leqslant 5$ (false discovery rate, FDR) between two groups.

In order to analyze jointly the miRNA and mRNA profiles of the fusion mass, we extracted 3′ UTR sequences of each porcine gene predicted from porcine genome from UCSC (University of California Santa Cruz) genome browser. Probe sets on porcine genome array were mapped to each porcine gene. Target genes for each miRNA were then predicted with miRanda program.

To obtain the insight into the kinetics of the gene regulation during the process of bone formation in each group, clustering of self-organizing maps (SOMs) was performed by Multi Experiment Viewer 4.6.1 [16]. The expressed genes targeted by differentially miRNAs were mapped to Kyoto Encyclopedia of Genes and Genomes (KEGG) pathways based on the human accession id, using MAS (molecule annotation system, http://bioinfo.capitalbio.com/mas) platform. KEGG pathways with FDR-corrected P values less than 0.05 were considered statistically significant.

3 Results

3.1 Animal data

One pig from the 8-week observation time point was excluded from the analysis due to severe infection at a late stage of the observation period. The remaining 17 pigs went through the observation period without major complications. Histological evaluations demonstrated longitudinally bone trabeculae formed in the cages of BPE, rhBMP-2 and autograft samples. At the end of the 8-week observation period, the histological images in three groups looked nearly identical (Fig. 1).

3.2 Differentially expressed miRNAs and genes between BPE, rhBMP-2 and autograft

We compared miRNA and gene-expression ratios for the rhBMP-2/BPE, BPE/autograft, and rhBMP-2/autograft at each time point to identify the magnitudes of the transcriptional responses among them (Table 1). In order to investigate different bone graft substitutes activated the miRNAs in the regulation of bone regeneration, we attempted to predict potential targeted genes of the differentially expressed miRNAs. Putative targets of each miRNA were comparatively analyzed with the gene-expression profiles according to the negative regulation mechanism of miRNAs (Table 2). Several miRNAs participated in the regulation of the immune and inflammation response at the early postoperative stage, including let-7, miR-129, miR-21, miR-133, miR-140, miR-146, miR-184, and miR-224. At 2 weeks, miR-129 and miR-133 in rhBMP-2 and BPE groups were different from autograft group, which targeted inflammation-related genes such as CD45 antigen isoform 1 precursor, alveolar macrophage-derived chemotactic factor-I, CD59, CD2, chemokine (C–X–C motif) ligand 2, etc. There was a little evidence characterized the regulation of targeted inflammation-related genes only in BPE group. At 8 weeks, few inflammation-related gene regulated by miRNAs was different between autograft group and other two groups.

At the later postoperative stage, there existed some miRNAs, such as miR-19, miR-29, miR-140, miR-181, miR-218, miR-363, and miR-374, mainly in regulation of bone regeneration related-genes. At 8 weeks, miR-181, miR-29 and miR-363 in rhBMP-2 group were different from autograft group, which targeted osteogenetic genes such as calcitonin receptor, type I collagen-α2, type I collagen-α1, etc.

3.3 Co-expressed miRNAs and genes among BPE, rhBMP-2 and autograft

To obtain the insight into the kinetics of the miRNAs and genes during the process of bone formation in each group,

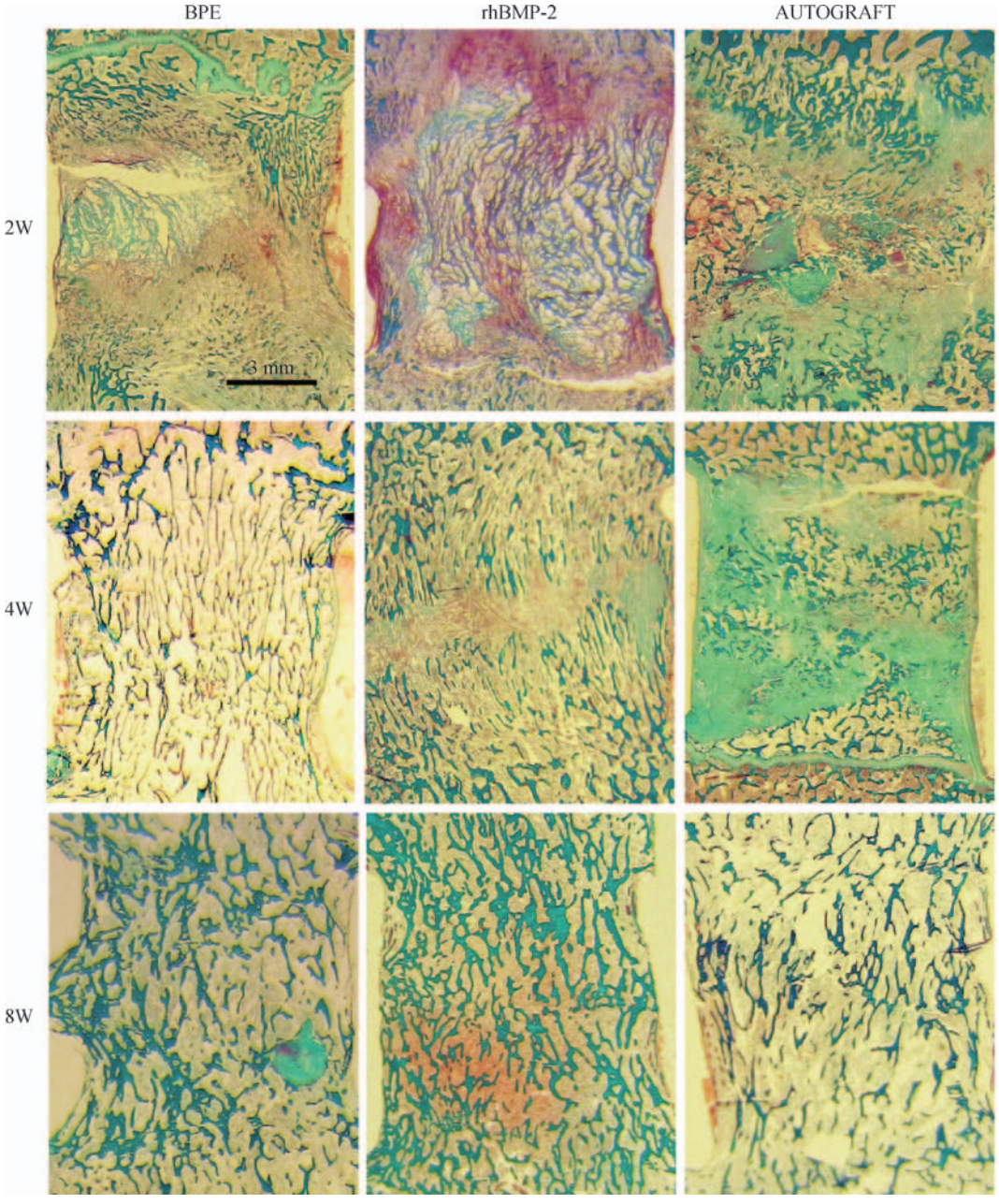

Fig. 1 Micrographs from histologic sections of the graft plugs taken out from the cages filled with BPE, rhBMP-2 and AUTOGRAFT in the pigs that had been killed at 2, 4 and 8 weeks. New bone formation can already be seen inside the plugs as early as 4 weeks. BPE, equine bone protein extracts; rhBMP-2, recombinant human bone morphogenetic protein-2/absorbable collagen sponge; AUTOGRAFT, autograft bone. Staining: Goldners-Trichrome.

the co-expressed miRNAs and genes in each group at 2, 4 and 8 weeks were irrespectively organized into 4 clusters, including up-down, up-up, down-up, and down-down cluster, using SOM analysis (Fig. 2). We attempted to predict potential targeted genes of the co-expressed miRNAs. Putative targets of each miRNA were compared with the co-expressed genes profiles according to the negative regulation mechanism of miRNAs (Table 3).

3.4 Assigning expressed genes targeted by differentially miRNAs to known pathways

To facilitate the biological interpretation of screened genes, we performed KEGG analyses using the genes targeted by differentially miRNAs expressed either between BPE, rhBMP-2 and autograft or within the time course. Notably, many KEGG pathways associated with immune and

inflammation responses were up-regulated in early time course in BPE and rhBMP-2 groups, compared with autograft groups. These included leukocyte transendothelial migration, cell adhesion molecules, mammalian target of rapamycin (mTOR) signaling pathway, cytokine–cytokine receptor interaction, complement and coagulation cascades, Toll-like receptor (TLR) signaling pathway, and complement and coagulation cascades (Table 4).

Table 1 The numbers of genes and miRNAs compared between two bone substitutes at different time points

Comparing group	Time point	Number			
		miRNA Upregulation [a)]	Gene Downregulation [b)]	miRNA Downregulation [b)]	Gene Upregulation [a)]
BPE/rhBMP-2	2w	1	696	5	408
	4w	12	338	1	107
	8w	8	479	5	244
BPE/AUTOGRAFT	2w	6	364	2	259
	4w	1	356	7	177
	8w	3	310	1	843
rhBMP-2/AUTOGRAFT	2w	6	149	2	178
	4w	7	39	2	69
	8w	2	62	11	504

a) Upregulation: ratio⩾2.
b) Downregulation: ratio⩽−2.
Note: BPE, equine bone protein extract; rhBMP-2, recombinant human bone morphogenetic protein-2/absorbable collagen sponge; AUTOGRAFT, autograft bone.

Table 2 Differentially expressed miRNAs and targeted genes between rhBMP-2, BPE and AUTOGRAFT

Comparing group	miRNA	Ratio	Targeted gene	Ratio
BPE/rhBMP-2 (2w)	miR-146	2.84	microseminoprotein, beta	−2
			histone H3.3A	−2.04
			lysozyme	−2.44
			uncoupling protein 2	−2.73
			CD45 antigen isoform 1 precursor	−2.88
			RANTES protein	−3.16
			monocyte chemoattractant protein 1	−4.99
			CD3g molecule, gamma (CD3-TCR complex)	−8.26
	miR-129	−2.08	dickkopf homolog 3	3.22
			disintegrin-metalloproteinase precursor	2.66
			glycoprotein GPIIIa	2.51
	miR-486	−2.5	unc-5 homolog C (C. elegans)	2.5
BPE/AUTOGRAFT (2w)	miR-129	2.79	CD45 antigen isoform 1 precursor	−2.22
			ameloblastin	−2.31
			histone H3.3A	−5.01
			alveolar macrophage-derived chemotactic factor-I	−5.06
	miR-210	2.16	angiopoietin-like 4	−3.98
	miR-133	−3.11	RAN, member RAS oncogene family	4.94
			microsomal prostaglandin E synthase-1	4.08
			destrin	2.73
			CD59 molecule, complement regulatory protein	2.27
rhBMP-2/AUTOGRAFT (2w)	miR-129	4.81	neuron-derived orphan receptor-1 alfa	−2.32
			chemokine (C–X–C motif) ligand 2	−2.85
			histone H3.3A	−7.01
			alveolar macrophage-derived chemotactic factor-I	−8.87
	miR-140	2.34	Toll-like receptor 4	−2.1
			glutamate-ammonia ligase (glutamine synthetase)	−2.11
			vascular endothelial growth factor	−2.36
	miR-133	−2.04	CD2 molecule	2.15
	miR-206	−2.05	cyclin D2	2.43

(*Continued*)

Comparing group	miRNA	Ratio	Targeted gene	Ratio
BPE/rhBMP-2 (4w)	let-7	2.43	alveolar macrophage-derived chemotactic factor-II	−7.55
	miR-21	2.39	vinculin	−2.51
			interleukin 1, beta	−2.77
			superoxide dismutase 2, mitochondrial	−3.42
			translationally controlled tumor protein	−4.77
	miR-129	2.39	pleiotrophic factor beta	−3.27
			chemokine (C–X–C motif) ligand 2	−3.94
			histone H3.3A	−4.5
			alveolar macrophage-derived chemotactic factor-I	−7.04
	miR-133	4.01	smooth muscle protein 22-alpha	−2.35
			selectin E (endothelial adhesion molecule 1)	−2.74
			MOESIN protein	−2.77
			interleukin 1, beta	−3.51
			alveolar macrophage-derived chemotactic factor-II	−6.63
			alveolar macrophage-derived chemotactic factor-II	−7.55
	miR-140	7.10	protein phosphatase 1, regulatory (inhibitor) subunit 12A	−2.05
			vinculin	−2.51
			Toll-like receptor 4	−2.55
	miR-142	2.51	exportin 1 (CRM1 homolog, yeast)	−2.07
			phorbol-12-myristate-13-acetate-induced protein 1	−2.3
	miR-184	2.69	Toll-like receptor 4	−2.55
			superoxide dismutase 2, mitochondrial	−3.42
	miR-224	3.56	interleukin 1 receptor antagonist	−3.8
	miR-374	2.16	hyaluronan and proteoglycan link protein 1	−4.79
BPE/AUTOGRAFT (4w)	miR-129	2.80	chemokine (C–X–C motif) ligand 2	−2.04
			prostaglandin F receptor (FP)	−2.07
			interleukin 13 receptor, alpha 1	−2.16
			alveolar macrophage-derived chemotactic factor-I	−3.23
			pleiotrophic factor beta	−4.44
	miR-133	2.92	CD59 molecule, complement regulatory protein	−2.02
			selectin E (endothelial adhesion molecule 1)	−2.26
			MOESIN protein	−2.52
			interleukin 1, beta	−2.94
			smooth muscle protein 22-alpha	−3.1
	miR-184	2.27	superoxide dismutase 2, mitochondrial	−2.69
	miR-206	3.44	fibronectin	−2.11
	miR-218	2.45	glutamine-fructose-6-phosphate transaminase 1	−2.11
			neuropeptide Y receptor Y1	−2.36
			hyaluronan and proteoglycan link protein 1	−5.72
rhBMP-2/AUTOGRAFT (4w)	miR-224	−4.54	interleukin 1 receptor antagonist	3.71
	miR-935	−2.27	histone H3.3A	2.42
BPE/rhBMP-2 (8w)	let-7	2.34	alveolar macrophage-derived chemotactic factor-II	−2.09
	miR-19	2.24	insulin-like growth factor binding protein 3	−2.18
	miR-21	3.33	translationally controlled tumor protein	−3.27
			platelet basic protein	−13.7
	miR-129	8.18	topoisomersae II	−3.44
			alveolar macrophage-derived chemotactic factor-I	−3.52
	miR-335	2.02	translationally controlled tumor protein	−3.27
	miR-133	−2.32	microsomal prostaglandin E synthase-1	3.35
			CD59 molecule, complement regulatory protein	2.26
			angiopoietin-like 4	2.16
	miR-139	−2.07	neuron-derived orphan receptor-1 alfa	2.07
	miR-181	−2.91	coxsackie-adenovirus-receptor homolog	2.19
			neuron-derived orphan receptor-1 alfa	2.07
			leukemia inhibitory factor	2.06

(*Continued*)

Comparing group	miRNA	Ratio	Targeted gene	Ratio
BPE/AUTOGRAFT (8w)	miR-181	2.17	ST8 alpha-N-acetyl-neuraminide alpha-2,8-sialyltransferase 4	−2.13
			O-linked N-acetylglucosamine (GlcNAc) transferase (UDP-N-acetylglucosamine:polypeptide-N-acetylglucosaminyl transferase)	−2.23
			CD47 antigen/integrin-associated protein	-4.02
			hydroxymethylbilane synthase	-4.55
	miR-218	−2.34	v-kit Hardy-Zuckerman 4 feline sarcoma viral oncogene homolog	2.75
			glutamine-fructose-6-phosphate transaminase 1	2.75
			calumenin	2.48
			insulin-like growth factor 2 (somatomedin A)	2.24
rhBMP-2/AUTOGRAFT (8w)	miR-181	6.34	calcitonin receptor	−2.35
			ST8 alpha-N-acetyl-neuraminide alpha-2,8-sialyltransferase 4	−2.46
			CD47 antigen/integrin-associated protein	−2.72
	let-7	−2.90	interferon-related developmental regulator 1	2.5
			splicing factor, arginine/serine-rich 11	2.25
			acyl-CoA synthetase long-chain family member 4	2.2
	miR-10	−2.49	splicing factor, arginine/serine-rich 10 (transformer 2 homolog, Drosophila)	2.71
			scavenger receptor class B member 2	2.01
	miR-19	−2.03	chemokine (C–X–C motif) ligand 12 (stromal cell-derived factor 1)	4.51
			protein phosphatase 1, regulatory (inhibitor) subunit 12A	4.05
			RAB14, member RAS oncogene family	3.19
			v-kit Hardy-Zuckerman 4 feline sarcoma viral oncogene homolog	2.49
			karyopherin alpha 3	2.3
			acyl-CoA synthetase long-chain family member 4	2.2
	miR-21	−3.03	Janus kinase 2	2.81
			superoxide dismutase 2, mitochondrial	2.58
	miR-29	−2.56	collagen, type I, alpha 2	3.19
			RAB14, member RAS oncogene family	3.19
			calumenin	2.86
			splicing factor, arginine/serine-rich 10 (transformer 2 homolog, Drosophila)	2.71
			hyaluronan and proteoglycan link protein 1	2.41
			tropomodulin 3 (ubiquitous)	2.32
			lipoprotein lipase	2.28
			ROD1 regulator of differentiation 1	2.25
			parathyroid hormone-like hormone	2.24
			collagen, type I, alpha 1	2.02
	miR-129	−5.37	Janus kinase 2	2.81
			interleukin 13 receptor, alpha 1	2.79
			interferon-related developmental regulator 1	2.5
			acyl-CoA synthetase long-chain family member 4	2.2
	miR-140	−5.93	protein phosphatase 1, regulatory (inhibitor) subunit 12A	4.05
			calumenin	2.86
			ROD1 regulator of differentiation 1	2.25
	miR-363	−2.14	collagen, type I, alpha 2	3.45
			serine/threonine kinase 6	2.12
	miR-374	−2.38	polypyrimidine tract-binding protein	4.41
			calumenin	2.86
			splicing factor, arginine/serine-rich 10 (transformer 2 homolog, Drosophila)	2.71
			endosulfine alpha	2.51
			interferon-related developmental regulator 1	2.5
			hyaluronan and proteoglycan link protein 1	2.41
			ubiquitin-conjugating enzyme E2, J1	2.38
			acyl-CoA synthetase long-chain family member 4	2.2
			cyclin B	2.06

Note: BPE, equine bone protein extract; rhBMP-2, recombinant human bone morphogenetic protein-2/absorbable collagen sponge; AUTOGRAFT, autograft bone.

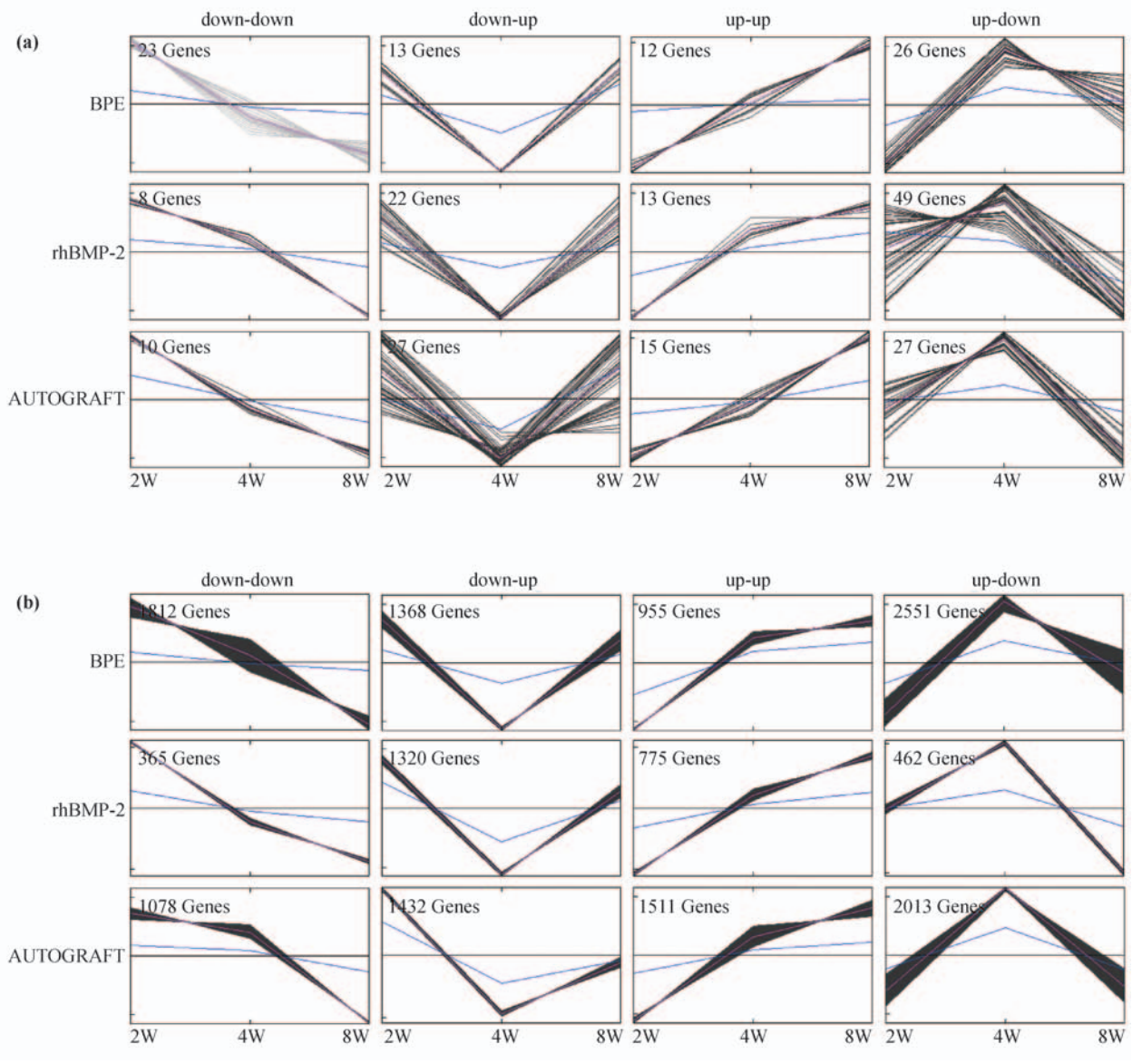

Fig. 2 Self-organizing maps of the co-expressed miRNAs and genes in each group. All different miRNAs and genes were irrespectively organized into 4 clusters according to the up or down regulation of the miRNAs and genes at different time point, including up-down, up-up, down-up, and down-down clusters. These maps demonstrated time sequential changes of differentially expressed miRNAs and genes during the process of anterior lumbar interbody fusion using equine bone protein extract, rhBMP-2 and autograft. **(a)** Self-organizing maps of the co-expressed miRNAs. **(b)** Self-organizing maps of the co-expressed genes. BPE, equine bone protein extracts; rhBMP-2, recombinant human bone morphogenetic protein-2/absorbable collagen sponge; AUTOGRAFT, autograft bone.

4 Discussion

miRNAs are known to play important roles in the epigenetic regulation for individual development, stem cell differentiation and human diseases. miRNAs, triggered by different bone graft biomaterials *in vitro*, were also verified to regulate bone formation [3–12]. So far, the exact mechanisms involved are still mysterious, but the likelihood that bone regeneration *in vivo* with the bone graft biomaterials is initiated at the level of genes suggests that a novel mechanism with miRNA-mediated regulation existed. Using miRNA microarray technique, we found time sequential changes of differentially expressed miRNAs during the process of an ALIF model in pigs using equine BPE, rhBMP-2 and autograft bone. By means of jointly analyzed miRNA and mRNA profiles of fusion mass, we demonstrated important roles of miRNAs in balancing the inflammation and bone formation after different bone graft biomaterials were implanted in an ALIF model in pig.

Table 3 Co-expressed miRNAs and genes among rhBMP-2, BPE and AUTOGRAFT

Cluster	miRNA	Targeted gene
Down-up	miR-26	ryanodine receptor 3
		kruppel-like factor 4
		SMAD family member 4
		zinc finger protein, X-linked
		BH3 interacting domain death agonist
		collagen, type V, alpha 1
	miR-320	transcription factor AP-2 beta
		ryanodine receptor 3
		SMAD family member 4
	miR-424	SMAD family member 4
		interleukin 1, beta
		heat shock 27kDa protein 1
		CD47 antigen/integrin-associated protein
		ADP-ribosylation factor-like protein 3
		putative MIP-1beta protein
	miR-664	gelatinase A
		ADP-ribosylation factor-like 1
		SMAD family member 4
Up-down	miR-22	estrogen receptor 1
		nuclear receptor coactivator 1
		5-hydroxytryptamine (serotonin) receptor 2C
	miR-23	5-hydroxytryptamine (serotonin) receptor 2C
		nuclear receptor coactivator 1
	miR-30	phosphoglucomutase 1
		leukemia inhibitory factor receptor
		occludin
	miR-146	phosphoglucomutase 1
		C-reactive protein
		polo-like kinase 2 (Drosophila)
	miR-181	glycerol-3-phosphate dehydrogenase
		neuron-derived orphan receptor-1 alfa
		early growth response protein 1 (Egr-1, NGFI-A)
		estrogen receptor 1
		tubulin tyrosine ligase

Note: BPE, equine bone protein extracts; rhBMP-2, recombinant human bone morphogenetic protein-2/absorbable collagen sponge; AUTOGRAFT, autograft bone.

Inflammation is a highly regulated biological response that plays an immediate and crucial role in promoting regeneration after bone fracture or injury [17–19]. A growing body of evidence has emerged that a complex balance exists between bone tissue and the immune system, which is responsible for the inflammatory response, and that obliterating inflammation has also damaging effects on bone healing [18,20–21]. Therefore, how to maintain a certain degree of inflammation is one of key factors on bone formation. In the present study, we found that miRNA could make some contributions to maintaining dynamic balance of inflammation in different bone graft biomaterials. At the early postoperative stage, several miRNAs, including let-7, miR-129, miR-21, miR-133, miR-140, miR-146, miR-184, and miR-224, were thought to regulate the immune and inflammation response. Most of their targeted genes related to inflammatory response were inversely expressed, such as CD45 antigen isoform 1 precursor [22], alveolar macrophage-derived chemotactic factor-I [23–24], CD59 [25], CD2 [26], chemokine (C–X–C motif) ligand 2 [27]. These results suggested that different immunogenicity of three bone graft biomaterials induced vary cytokines to activate different degree of inflammation response, which provided suitable inflam-

matory microenvironment for bone formation. These findings were in line with the studies of miRNAs in tumor [28–30].

In our previous studies, authors showed that two different kinds of molecular mechanisms of bone formation with three bone graft biomaterials, e.g., endochondral ossification in equine BPE and autograft bone, and intramembranous ossification in rhBMP-2 [15]. Although we cannot provide the evidence that miRNAs regulate endochondral and intramembranous ossification in the present study, miRNAs may involve other regulation mechanism of bone formation. Several genes involved bone formation such as calcitonin receptor [31], type I collagen-α2 [32], type I collagen-α1 [33] were targeted by miR-181, miR-29 and miR-363. Among these miRNAs, miR-29 has been verified to modulate Wnt signaling in

Table 4 KEGG pathways between rhBMP-2, BPE and AUTOGRAFT gene targeted by different miRNAs expression

Comparing group	Comparing group	*p*-Value	*q*-Value
BPE/rhBMP-2 (2w)	T cell receptor signaling pathway	0.008	0.012
	hematopoietic cell lineage	0.012	0.012
	ECM-receptor interaction	0.003	0.006
	regulation of actin cytoskeleton	0.007	0.006
	focal adhesion	0.009	0.006
	hematopoietic cell lineage	0.012	0.006
BPE/AUTOGRAFT (2w)	complement and coagulation cascades	0.008	0.012
	hematopoietic cell lineage	0.012	0.012
	leukocyte transendothelial migration	0.006	0.006
rhBMP-2/BPE (2w)	leukocyte transendothelial migration	0.006	0.006
	cell adhesion molecules (CAMs)	0.009	0.012
	hematopoietic cell lineage	0.012	0.012
	peptidoglycan biosynthesis	0.001	0.002
	nitrogen metabolism	0.001	0.002
	mTOR signaling pathway	0.004	0.002
	glutamate metabolism	0.005	0.003
	focal adhesion	0.018	0.007
	cell cycle	0.004	0.006
	Wnt signaling pathway	0.006	0.006
	focal adhesion	0.009	0.006
	Jak-STAT signaling pathway	0.016	0.008
BPE/INFUSE (4w)	adherens junction	0.006	0.005
	Toll-like receptor signaling pathway	0.012	0.005
	type I diabetes mellitus	0.012	0.005
	leukocyte transendothelial migration	0.012	0.005
	regulation of actin cytoskeleton	0.014	0.005
	apoptosis	0.015	0.005
	focal adhesion	0.018	0.005
	MAPK signaling pathway	0.018	0.005
	hematopoietic cell lineage	0.023	0.005
	cytokine-cytokine receptor interaction	0.041	0.008
	leukocyte transendothelial migration	0.006	0.006
	Toll-like receptor signaling pathway	0.018	0.008
	type I diabetes mellitus	0.018	0.008
	leukocyte transendothelial migration	0.019	0.008
	regulation of actin cytoskeleton	0.021	0.008
	apoptosis	0.022	0.008
	cell adhesion molecules (CAMs)	0.027	0.008
	MAPK signaling pathway	0.027	0.008
	hematopoietic cell lineage	0.035	0.009
	cytokine–cytokine receptor interaction	0.062	0.014

(*Continued*)

Comparing group	Comparing group	*p*-Value	*q*-Value
BPE/AUTOGRAFT (4w)	leukocyte transendothelial migration	0.019	0.028
	calcium signaling pathway	0.033	0.028
	Jak-STAT signaling pathway	0.048	0.028
	cytokine-cytokine receptor interaction	0.062	0.028
	neuroactive ligand-receptor interaction	0.069	0.028
	hematopoietic cell lineage	0.001	0.002
	Toll-like receptor signaling pathway	0.023	0.009
	type I diabetes mellitus	0.023	0.009
	leukocyte transendothelial migration	0.025	0.009
	regulation of actin cytoskeleton	0.028	0.009
	apoptosis	0.029	0.009
	complement and coagulation cascades	0.032	0.009
	cell adhesion molecules (CAMs)	0.036	0.009
	MAPK signaling pathway	0.036	0.009
	cytokine-cytokine receptor interaction	0.081	0.016
	neuroactive ligand-receptor interaction	0.024	0.024
rhBMP-2/BPE (4w)	–	–	–
BPE/rhBMP-2 (8w)	leukocyte transendothelial migration	0.006	0.006
	complement and coagulation cascades	0.008	0.012
	hematopoietic cell lineage	0.012	0.012
	Jak-STAT signaling pathway	0.016	0.021
	cytokine-cytokine receptor interaction	0.021	0.021
BPE/AUTOGRAFT (8w)	ECM-receptor interaction	0.003	0.003
rhBMP-2/BPE (8w)	ECM-receptor interaction	0.007	0.013
	neuroactive ligand-receptor interaction	0.046	0.046
	fatty acid metabolism	0.004	0.007
	adipocytokine signaling pathway	0.007	0.007
	fatty acid metabolism	0.008	0.009
	leukocyte transendothelial migration	0.012	0.009
	adipocytokine signaling pathway	0.013	0.009
	adipocytokine signaling pathway	0.007	0.013
	Jak-STAT signaling pathway	0.016	0.016
	Alzheimer's disease	0.001	0.002
	glycerolipid metabolism	0.002	0.002
	fatty acid metabolism	0.004	0.007
	adipocytokine signaling pathway	0.007	0.007

Note: BPE, equine bone protein extracts; rhBMP-2, recombinant human bone morphogenetic protein-2/absorbable collagen sponge; AUTOGRAFT, autograft bone.

human osteoblasts through target three inhibitors of Wnt signaling, Dkk1 (dikkopf-1), Kremen2 (kringle domain-containing transmembrane protein), and sFRP2 (secreted frizzled-related protein 2), which formed a positive feed-back loop [34–35].

SMAD4, a common intracellular mediator for the canonical transforming growth factor/bone morphogenetic protein (TGF/BMP) signaling pathway, plays a crucial role in regulating organogenesis. There were many evidences to suggest that the TGF/BMP and Wnt signaling pathways regulated one another synergistically or antagonistically in organogenesis such as bone [36–37], joint [38], hair [39], intestine [40] and tooth [41]. As a mediator between TGF and BMP signaling pathways, SMAD4 could also upregulate Dkk1 and sFRP2 and downregulate Wnt signaling pathway [41]. In this study, SMAD4 was targeted by four miRNAs including miR-26, miR-320, miR-424 and miR-664, suggested that miRNAs may maintain a balance between the TGF/BMP and Wnt signaling pathways for bone formation.

One of the limitations in the present study was that all the samples for microarrays took from intervertebral fusion mass, therefore, it is difficult to know a relevant miRNA and targeted genes involved in which kind of cell type.

However, this study was an overview of the miRNAs' expression in regulating the inflammation and bone formation. Another limitation is that the bone graft substitutes material just limited in BPE, rhBMP-2, and autograft bone, although bone morphogenetic protein was the most promising currently bone substitutes materials both in preclinical study [42–46] and clinical application [47]. Further study should extend to other materials.

5 Conclusions

To conclude, the findings in the present study demonstrate the important roles of miRNAs in balancing the inflammation and bone formation after different bone graft biomaterials were implanted in an ALIF model in pigs. At the early postoperative stage, miRNAs, including let-7, miR-129, miR-21, miR-133, miR-140, miR-146, miR-184, and miR-224, are involved in the regulation of the immune and inflammation response, which provided suitable inflammatory microenvironment for bone formation. At the late stage, several miRNAs directly regulate SMAD4, estrogen receptor 1 and 5-hydroxytryptamine (serotonin) receptor 2C for bone formation.

Abbreviations

ACS	absorbable collagen sponge
ALIF	anterior lumbar interbody fusion
BMP	bone morphogenetic protein
BPE	bone protein extract
CAM	cell adhesion molecule
dNTP	deoxyribonucleoside triphosphate
FDR	false discovery rate
KEGG	Kyoto Encyclopedia of Genes and Genomes
miRNA	microRNA
mRNA	messenger RNA
mTOR	mammalian target of rapamycin
OD	optical density
PEEK	polyetheretherketone
PMMA	polymethyl methacrylate
rhBMP	recombinant human bone morphogenetic protein
SAM	Significance Analysis of Microarrays
sFRP	secreted frizzled-related protein
SOM	self-organizing map
TGF	transforming growth factor
TLR	Toll-like receptor
UTR	untranslated region

Acknowledgements The present study was financially supported by National Program on Key Basic Research Project (973 Program; Grant No. 2012CB619100), China Postdoctoral Science Foundation (Grant No. 2013M531876), the National Natural Science Foundation of China (Grant Nos. U0732001, 81000676, 81171682 and 81071512), the Fabrikant Mads Clausens Foundation, Sino-Danish Science and Technology Cooperation Project between Chinese and Danish Governments (AM14:29NNP14), Scientific Research Foundation for the Returned Overseas Chinese Scholars by State Education Ministry (Grant Nos. 2009-136 and 2011-508), Ph.D. Programs Foundation of Ministry of Education of China (Grant No. 20100171110054), and the High-level Talented People Project for Higher Education Institutions of Guangdong Province (Grant No. 80000-3210002). Ossacur AG (Oberstenfeld, Germary) provided free supply of COLLOSS® E. The authors would like to thank the Orthopaedic Research Laboratory and the Institute of Clinical Medicine at Aarhus University, the staff at the CapitalBio Incorporation of Beijing, China for their assistance during the entire project.

References

[1] Hobert O. Gene regulation by transcription factors and microRNAs. Science, 2008, 319(5871): 1785–1786

[2] Lian J B, Stein G S, van Wijnen A J, et al. MicroRNA control of bone formation and homeostasis. Nature Reviews Endocrinology, 2012, 8(4): 212–227

[3] Palmieri A, Pezzetti F, Brunelli G, et al. Anorganic bovine bone (Bio-Oss) regulates miRNA of osteoblast-like cells. The International Journal of Periodontics & Restorative Dentistry, 2010, 30 (1): 83–87

[4] Palmieri A, Pezzetti F, Avantaggiato A, et al. Titanium acts on osteoblast translational process. Journal of Oral Implantology, 2008, 34(4): 190–195

[5] Palmieri A, Brunelli G, Guerzoni L, et al. Comparison between titanium and anatase miRNAs regulation. Nanomedicine, 2007, 3 (2): 138–143

[6] Palmieri A, Pezzetti F, Brunelli G, et al. Anatase nanosurface regulates microRNAs. The Journal of Craniofacial Surgery, 2008, 19(2): 328–333

[7] Palmieri A, Pezzetti F, Brunelli G, et al. Short-period effects of zirconia and titanium on osteoblast microRNAs. Clinical Implant Dentistry and Related Research, 2008, 10(3): 200–205

[8] Palmieri A, Pezzetti F, Spinelli G, et al. PerioGlas regulates osteoblast RNA interfering. Journal of Prosthodontics, 2008, 17 (7): 522–526

[9] Palmieri A, Pezzetti F, Brunelli G, et al. Differences in osteoblast miRNA induced by cell binding domain of collagen and silicate-based synthetic bone. Journal of Biomedical Science, 2007, 14(6): 777–782

[10] Palmieri A, Pezzetti F, Brunelli G, et al. Calcium sulfate acts on the miRNA of MG63E osteoblast-like cells. Journal of Biomedical Materials Research Part B: Applied Biomaterials, 2008, 84B(2): 369–374

[11] Palmieri A, Pezzetti F, Brunelli G, et al. Zirconium oxide regulates RNA interfering of osteoblast-like cells. Journal of Materials Science: Materials in Medicine, 2008, 19(6): 2471–2476

[12] Palmieri A, Pezzetti F, Brunelli G, et al. Medpor regulates osteoblast's microRNAs. Bio-Medical Materials and Engineering, 2008, 18(2): 91–97

[13] Foldager C, Bendtsen M, Zou X, et al. ISSLS prize winner: positron emission tomography and magnetic resonance imaging for monitoring interbody fusion with equine bone protein extract, recombinant human bone morphogenetic protein-2, and autograft. Spine, 2008, 33(25): 2683–2690

[14] Li H, Zou X, Woo C, et al. Experimental anterior lumbar interbody fusion with an osteoinductive bovine bone collagen extract. Spine, 2005, 30(8): 890–896

[15] Zou X, Zou L, Foldager C, et al. Different mechanisms of spinal fusion using equine bone protein extract, rhBMP-2 and autograft during the process of anterior lumbar interbody fusion. Biomaterials, 2009, 30(6): 991–1004

[16] Saeed A I, Sharov V, White J, et al. TM4: a free, open-source system for microarray data management and analysis. BioTechniques, 2003, 34(2): 374–378

[17] Mountziaris P M, Spicer P P, Kasper F K, et al. Harnessing and modulating inflammation in strategies for bone regeneration. Tissue Engineering Part B: Reviews, 2011, 17(6): 393–402

[18] Mountziaris P M, Mikos A G. Modulation of the inflammatory response for enhanced bone tissue regeneration. Tissue Engineering Part B: Reviews, 2008, 14(2): 179–186

[19] Kolar P, Schmidt-Bleek K, Schell H, et al. The early fracture hematoma and its potential role in fracture healing. Tissue Engineering Part B: Reviews, 2010, 16(4): 427–434

[20] Takayanagi H. Osteoimmunology and the effects of the immune system on bone. Nature Reviews Rheumatology, 2009, 5(12): 667–676

[21] Pape H C, Marcucio R, Humphrey C, et al. Trauma-induced inflammation and fracture healing. Journal of Orthopaedic Trauma, 2010, 24(9): 522–525

[22] Rodig S J, Shahsafaei A, Li B, et al. The CD45 isoform B220 identifies select subsets of human B cells and B-cell lymphoproliferative disorders. Human Pathology, 2005, 36(1): 51–57

[23] Koarai A, Traves S L, Fenwick P S, et al. Expression of muscarinic receptors by human macrophages. The European Respiratory Journal, 2012, 39(3): 698–704

[24] Koarai A, Yanagisawa S, Sugiura H, et al. Cigarette smoke augments the expression and responses of toll-like receptor 3 in human macrophages. Respirology, 2012, 17(6): 1018–1025

[25] Miwa T, Zhou L, Maldonado M A, et al. Absence of CD59 exacerbates systemic autoimmunity in MRL/lpr mice. Journal of Immunology, 2012, 189(11): 5434–5441

[26] Kalland M E, Oberprieler N G, Vang T, et al. T cell-signaling network analysis reveals distinct differences between CD28 and CD2 costimulation responses in various subsets and in the MAPK pathway between resting and activated regulatory T cells. Journal of Immunology, 2011, 187(10): 5233–5245

[27] Rouault C, Pellegrinelli V, Schilch R, et al. Roles of chemokine ligand-2 (CXCL2) and neutrophils in influencing endothelial cell function and inflammation of human adipose tissue. Endocrinology, 2013, 154(3): 1069–1079

[28] Chou J, Werb Z. MicroRNAs play a big role in regulating ovarian cancer-associated fibroblasts and the tumor microenvironment. Cancer Discovery, 2012, 2(12): 1078–1080

[29] Melo S A, Kalluri R. miR-29b moulds the tumour microenvironment to repress metastasis. Nature Cell Biology, 2013, 15(2): 139–140

[30] Chou J, Lin J H, Brenot A, et al. GATA3 suppresses metastasis and modulates the tumour microenvironment by regulating microRNA-29b expression. Nature Cell Biology, 2013, 15(2): 201–213

[31] Tural S, Kara N, Alayli G, et al. Association between osteoporosis and polymorphisms of the bone Gla protein, estrogen receptor 1, collagen 1-A1 and calcitonin receptor genes in Turkish postmenopausal women. Gene, 2013, 515(1): 167–172

[32] Lindahl K, Rubin C J, Brändström H, et al. Heterozygosity for a coding SNP in COL1A2 confers a lower BMD and an increased stroke risk. Biochemical and Biophysical Research Communications, 2009, 384(4): 501–505

[33] Narisawa S, Yadav M C, Millán J L. *In vivo* overexpression of tissue-nonspecific alkaline phosphatase increases skeletal mineralization and affects the phosphorylation status of osteopontin. Journal of Bone and Mineral Research, 2013, 28(7): 1587–1598

[34] Kapinas K, Kessler C, Ricks T, et al. miR-29 modulates Wnt signaling in human osteoblasts through a positive feedback loop. The Journal of Biological Chemistry, 2010, 285(33): 25221–25231

[35] Li Z, Hassan M Q, Jafferji M, et al. Biological functions of miR-29b contribute to positive regulation of osteoblast differentiation. The Journal of Biological Chemistry, 2009, 284(23): 15676–15684

[36] Kamiya N, Kobayashi T, Mochida Y, et al. Wnt inhibitors Dkk1 and Sost are downstream targets of BMP signaling through the type IA receptor (BMPRIA) in osteoblasts. Journal of Bone and Mineral Research, 2010, 25(2): 200–210

[37] Kamiya N, Ye L, Kobayashi T, et al. BMP signaling negatively regulates bone mass through sclerostin by inhibiting the canonical Wnt pathway. Development, 2008, 135(22): 3801–3811

[38] Guo X, Day T F, Jiang X, et al. Wnt/β-catenin signaling is

sufficient and necessary for synovial joint formation. Genes & Development, 2004, 18(19): 2404–2417

[39] Zhang J, He X C, Tong W G, et al. Bone morphogenetic protein signaling inhibits hair follicle anagen induction by restricting epithelial stem/progenitor cell activation and expansion. Stem Cells, 2006, 24(12): 2826–2839

[40] He X C, Zhang J, Tong W G, et al. BMP signaling inhibits intestinal stem cell self-renewal through suppression of Wnt–β-catenin signaling. Nature Genetics, 2004, 36(10): 1117–1121

[41] Li J, Huang X, Xu X, et al. SMAD4-mediated WNT signaling controls the fate of cranial neural crest cells during tooth morphogenesis. Development, 2011, 138(10): 1977–1989

[42] Zhang H, Sucato D J, Welch R D. Recombinant human bone morphogenic protein-2-enhanced anterior spine fusion without bone encroachment into the spinal canal: a histomorphometric study in a thoracoscopically instrumented porcine model. Spine, 2005, 30(5): 512–518

[43] Damien C J, Grob D, Boden S D, et al. Purified bovine BMP extract and collagen for spine arthrodesis: preclinical safety and efficacy. Spine, 2002, 27(16S): S50–S58

[44] Sandhu H S, Khan S N. Animal models for preclinical assessment of bone morphogenetic proteins in the spine. Spine, 2002, 27 (16S): S32–S38

[45] Minamide A, Yoshida M, Kawakami M, et al. The use of cultured bone marrow cells in type I collagen gel and porous hydroxyapatite for posterolateral lumbar spine fusion. Spine, 2005, 30 (10): 1134–1138

[46] Kandziora F, Pflugmacher R, Scholz M, et al. Comparison of BMP-2 and combined IGF-I/TGF-ss1 application in a sheep cervical spine fusion model. European Spine Journal, 2002, 11(5): 482–493

[47] Burks M V, Nair L. Long-term effects of bone morphogenetic protein-based treatments in humans. Journal of Long-Term Effects of Medical Implants, 2010, 20(4): 277–293